M. N. Idris

DEVELOPMENT OF EMERGENCY RESPONSE TEMPLATE ON ACCIDENTAL RELEASES OF SPILLS OF FLUIDS IN AN EXISTING REFINERY PROCESS PLANT

idrismn@unimaid.edu.ng

Process Refining Technology and Sustainable Energy Development Group,
Department of Chemical Engineering,
University of Maiduguri, Borno State, Nigeria

Development of emergency response template on accidental releases of spills of fluids in an existing refinery process plant

*M. N. Idris[1], U. O. Danjuma[1] and N. J. Biragbara[2]
[1.]Process Refining Technology and Sustainable Energy Development Group,
Department of Chemical Engineering, University of Maiduguri, Borno State, Nigeria.
[2]Petroleum Technology Development Fund, PTDF, Abuja, Nigeria.

* Corresponding author email address: idrismn@unimaid.edu.ng

Abstract

The continuous effort to make our plant systems to be viable, safe, productive and more economical units for quality production remain the crux of this subject. An emergency response plan is a systematic procedure that lays out the series of steps during critical events, such as accident and fire emergencies to ensure personnel and employees safety and minimize the impact on equipments and plant facilities. A template format is a computational file used as a master guide for creating other similar occurrences or events for engineering purposes and process improvement. The accidental releases or spills of fluids in refinery process plants pose significant environmental risks and without a well-defined emergency response plan, such incidents usually lead to environmental pollution, health hazards, and economic losses. Therefore, the need to develop a comprehensive and tailored emergency response template for refinery plants to mitigate these risks: outline response procedures and techniques for combating the spills at a specific location, ensure effective and efficient response despite geographical challenges and identify potential equipment man power and other recourses necessary to implement a spill response template.

The significance of this studies are in its potential to enhance the preparedness and response capabilities of refinery process plants and by providing a standardized and well-structured emergency response template, the results from the study shall help to minimize the impact on the environment, protect human health, and ensure efficiency in removing containments and quality clean-up operations.

The final results of this study produce a well-structured and comprehensive emergency response template that can be readily implemented in existing refinery process plants. The template will outline clear procedures, roles, and responsibilities for responding to accidental releases or spills of fluids, thereby minimizing environmental impact and facilitating an efficient emergency response.

Keywords: Accident, oil and gas plant, emergency response, template

Introduction

Centrifugal pump is a type of a turbo machine in which mechanical energy is converted into pressure energy by means of centrifugal force acting on the fluid. The impeller is the revolving component of the centrifugal pump that transmits energy from the electric motor that drives the pump to the fluid being pumped by acceleration of the fluid outwards from the centre of rotation. Impellers are often composed of corrosive and non-corrosive materials which are cast iron, steel, bronze, brass, aluminium, or plastic. When the fluid's outward flow is limited by the pump casing, the impeller's velocity is converted to pressure. Short cylinders with an open outlet called an eye to accept incoming fluid, vanes to push the fluid radially, and a splined, keyed, or threaded hole to accommodate a drive-shaft are typical impellers. The impeller is housed in the diffuser (also known as the volute), which catches and channels the water off the impeller. With the help of centrifugal force, water enters the impeller's centre (eye) and exits the impeller. A low-pressure area is generated as water exits the impeller's eye, causing more water to flow into the eye. This is caused by atmospheric pressure and centrifugal force (Pradesh, 2017; Rajendran & Purushothaman, 2012).

The pump performance curves for centrifugal pumps are typically drawn with Flow on the horizontal axis and Head produced on the vertical axis. Efficiency, power, and NPSH required (explained later) are all traditionally shown versus flow on the vertical axis. Given the large quantity of electricity used by pumping systems, even little increases in pumping efficiency could result in huge cost savings of electricity. The pump, together with the motor, transmission drive, pipes, and valves, is one of the most inefficient components of a pumping system (Flows el at., 2019; Selamat 2018; Selamat et al., 2018).

The aim and objective of the studies are: to analyze the pressure, head and efficiency of the designed centrifugal pump impeller, to improve on the efficiency and reliability of a centrifugal pump impeller by changing the blade angle and the use of corrosive and non-corrosive fluids, experimental measurements to analyze the pressure fluctuation performance of a centrifugal pump impeller using CFD. The research justification is that centrifugal pumps are widely used for steam power plants, irrigations, water supply power plants, sewage, oil refineries, chemical plants, hydraulic power service, and food processing factories and others because of their suitability in practically any service. Therefore, it is very important to find out design parameters and working condition to yield optimal output and maximum efficiency and reliability with lowest power consumption.

2.0 Background Literatures

Pumps are hydraulic machines that convert mechanical energy into hydraulic energy (in the form of a pressure head) and mechanically move fluids (liquids, semi-liquids, gases, and occasionally slurries) from low to high pressure. Pumps are powered by a reciprocating or rotational mechanism. In the review of the literatures, several authors are been depicted as presented in Table 1.

Table 1 Summarised version of reviewed investigations

Author(s)	Investigation and Tank farm capacity	Research Benefits/Product storage	Remarks
Ji et al., 2016	Positive displacement pumps and rotor-dynamic pumps are the two main types of pumps	Manual operation, electricity, tidal power, engines, wind power, solar power, and hydraulic energy are all sources of energy used by pumps to do mechanical work for the transfer of	A positive displacement pump is a mechanical device that moves liquid from the suction side to the discharge side by changing the volume of the chamber in the

		fluid.	suction side to the discharge side mechanically
Karmokar, 2019	The fluid is drawn into the impeller, which captures it. When the impeller reaches its maximum acceleration and the fluid has exited the impeller, it flows over a vast region.	Pulse transmission improves fluid flow by following the curve of the impeller vanes from the impeller centre outwards. As a result, using the Bernoulli's principle, kinetic energy is converted to pressure energy.	When fluid is displaced from the delivery side of the pump, more fluid is sucked from suction side and thus fluid flow is created
Li et al., 2020	In contrast to a positive displacement pump, which moves a fluid by trapping a fixed amount of fluid and forcing the trapped volume into the pump's discharge?	A rotor-dynamic pump is a dynamic mechanism in which energy is continuously conveyed to the pumped liquid via a spinning impeller, propeller, or rotor.	A centrifugal pump transfers mechanical energy into pressure energy using a rotor-dynamic design.
Idris and Kois 2022	CFD code was used to simulate pump efficiency and validated by comparing the predicted data with real experimental studies.	The centrifugal pump was designed within the constraint of pumping at a flow rate of 0.040 m^3/s and at a pump head of between 55-70 m.	The modelled-system design calculations for the pump was drawn in SOLIDWOKS, and further developed in CFD modeller

The main parts of centrifugal pump are the impeller, casing, suction pipe, delivery pipe and those are explained hereunder as depicted in Figure 1.
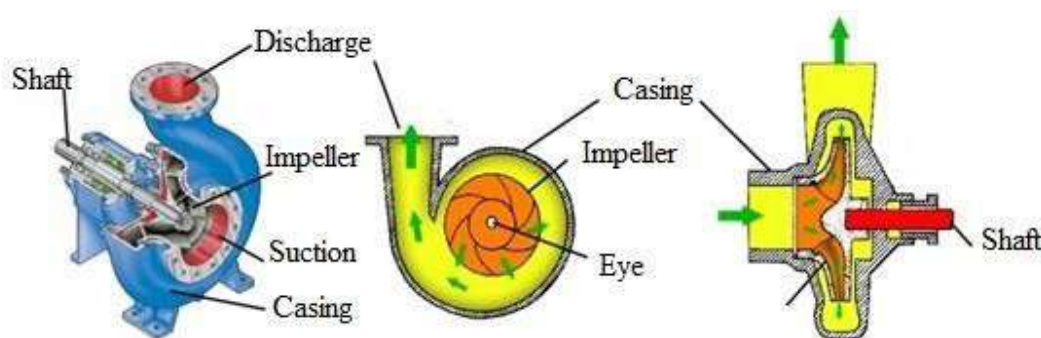

Figure 1: Centrifugal pump working principle

3.0   Materials and Methods

3.1   Materials: Commercial ANSYS software student version 2022.

Table 1 present the corrosive and non-corrosive fluid used in this study

Table 1: Corrosive and Non-corrosive fluids used

S/N	Corrosive		Non-corrosive	
	Fluid type	**Symbol**	**Fluid type**	**Symbol**
1	Saline Water	$x\text{H}_2\text{O}$	Water at 100^0C	H_2O
2	Hydrochloric acid	HCl	Gasoline	$n\text{CH}_4$
3	Methanol	CH_3OH	Kerosene	C_9H_{20}

Table 2: Density of different fluids

S/N	**Fluids**	**Symbol**	**Density (kg/m^3)**
1	Saline Water	$x\text{H}_2\text{O}$	1031
2	Hydrochloric acid	HCl	1169
3	Methanol	CH_3OH	792
4	Water at 100^0C	H_2O	993
5	Gasoline	$n\text{CH}_4$	720
6	Kerosene	C_9H_{20}	810

3.2 Method

3.2.1 Experimental Setup

Table 3: Specification of Centrifugal Pump Used.

Pump type	Head rise, H (m)	Discharge, Q (m^3/hr)	Pump speed, N (RPM)
H47 Centrifugal pump	20 - 120	144	2000

Table 4: Features of the centrifugal pump Impeller

S/N	**Parameters**	**Symbol**	**Values**
1.	Shaft diameter	D_s	40 mm
2.	Eye diameter	D_o	124 mm
3.	Hub diameter	D_h	106 mm
4.	Inlet diameter	D_1	125 mm
5.	Inlet blade width	b_1	54 mm
6.	Outlet blade width	b_2	30 mm
7.	Inlet blade angle	β_1	35°, 38°, 41°
8.	Outlet blade angle	β_2	47°, 50°, 53°

9.	Blade number	z	7	**Table 5:** Summary of calculated
10.	Blade thickness	t	16 mm	
11.	Outlet diameter	D_2	310 mm	

impeller data from BladeGen for various angles

S/N	Variables (m/s)	Impeller Inlet and Outlet Angles		
1		35^0-47^0	38^0-50^0	41^0-53^0
2	Cu_1	0.00	0.00	0.00
3	Cu_2	17.69	17.69	17.69
4	W_1	22.11	21.83	22.80
5	W_2	16.35	16.06	16.90
6	U_1	13.04	13.04	13.04
7	U_2	32.42	32.42	32.42
8	Cm_1	17.85	17.51	18.71

3.2.2 Analytical calculations for the blade inlet angle of 35° and outlet angle of 47° for the efficiencies of the existing design of impeller:

$$\text{Volumetric Efficiency } = \frac{1}{1+0.68(N)^{-\frac{Z}{S}}} = \frac{1}{1+0.68(2000)^{-\frac{67}{0.75}}} = 69.72\%$$

$$Hydraulic\ Efficiency = \frac{actual\ head\ of\ centrifugal\ pump}{total\ head\ of\ centrifugal\ pump} = \frac{50}{120} = 0.417 = 41.7\%$$

3.3 Design of Impeller to Improve Its Efficiency

The centrifugal pump impeller was created using Vista CPD (Centrifugal Pump Design) in ANSYS software, which was transferred to the BladeGen. The blade designed was viewed in the BladeGen. The mesh was auto generated in AM (ANSYS Meshing) using the platform in the ANSYS Workbench CFX which produced the most appropriate mesh for the analysis. The fillet was created in design modeler. The mesh was transferred to the CFX; Turbo wizard was used in CFX-Pre. The flow simulations were done in CFX-Solver within 100 iterations and all of the simulations were converged within 100 iterations. Hence, the results were viewed in CFD post (Turbo post). Final results were obtained in CFD post per boundary conditions given which gives accurate results of the analysis. The software calculator in CFD post gives the results of pressure, density, velocity and many more. The flow express is very important for performing CFD analysis which provided the results of fluids head, pressure, efficiency, pressure ration and many more.

4.0 Results and Discussions

4.1 Simulation Results

The impeller geometry was constructed in the ANSYS Workbench Vista CPD and the flow simulation was carried out using the ANSYS CFX. To initialize and run the simulation, a hybrid initialization was used to obtain the results. The results of the simulations were in terms of pressure contour and Vector velocity. After the analysis was carried out, the results were obtained from the software once the simulation has converged.

For the flow simulation, various corrosive liquids (Saline water, Hydrochloric acid and Methanol) and non-corrosive fluids (Water, Gasoline and Kerosene) at 2000rpm rotating speeds were selected for

different inlet and exit impeller angle of 35^0, 38^0, 41^0 and 47^0, 50^0, 53^0 respectively to be the variable factors in this project.

The results of the simulations were obtained from the CFD post software and compared among the three different inlet and outlet angle of impeller and the corrosive and non-corrosive working fluids. The input and output powers were calculated in order to obtain the impeller efficiency. The following results were taken in varying axis and cross section.

4.1.1 Impeller Designed
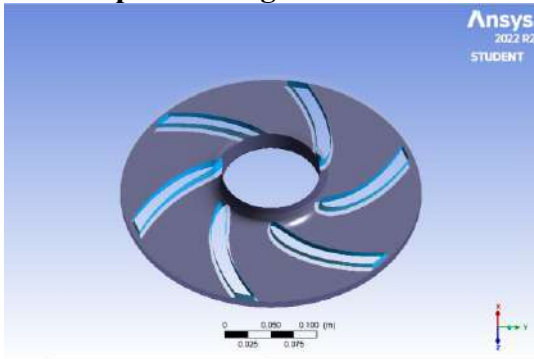
Figure 1: The designed model
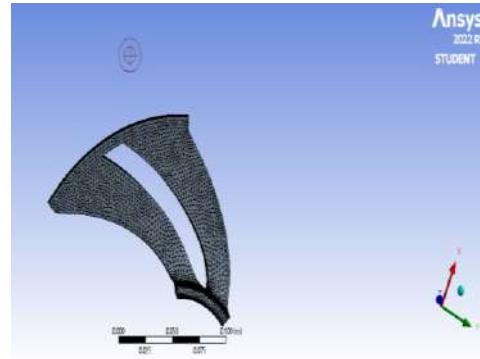
Figure 2: The Meshed Model
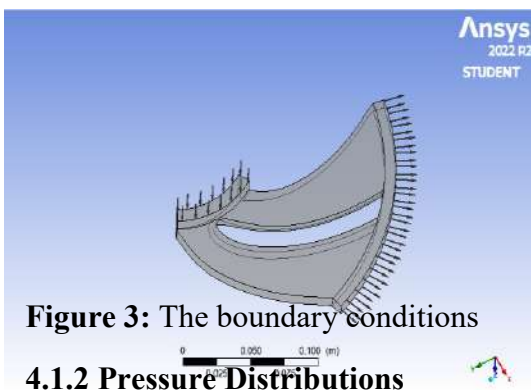
Figure 3: The boundary conditions

4.1.2 Pressure Distributions
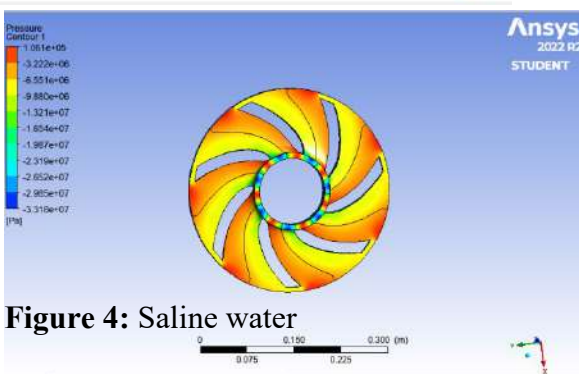
Figure 4: Saline water
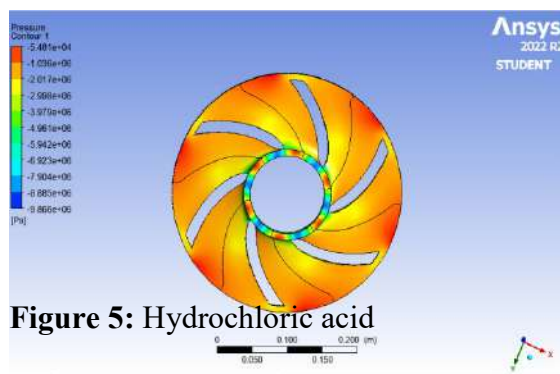
Figure 5: Hydrochloric acid
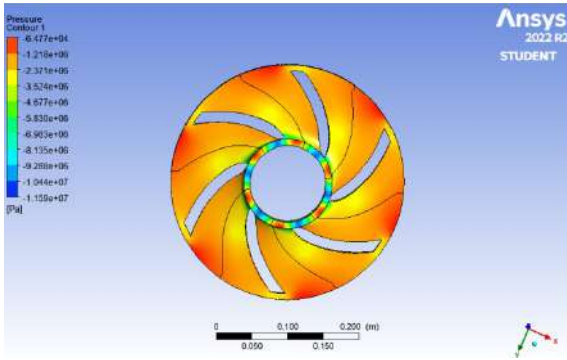
Figure 6: Methanol

Figures 4 – 6 depicts the pressure distribution across the impeller inlet angle of 35^0 and exit angle of 47^0 for various corrosive fluids.
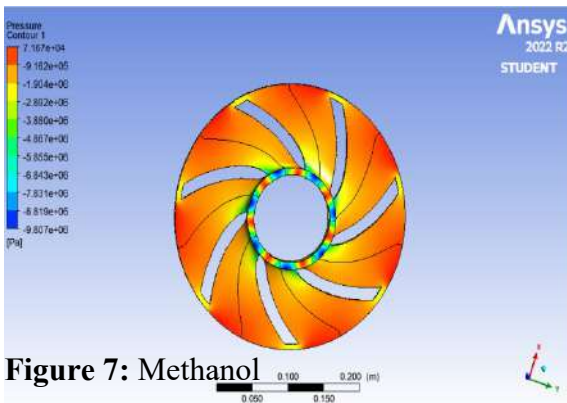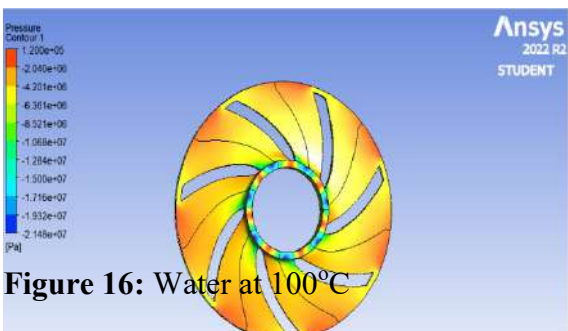

Figure 7: Methanol
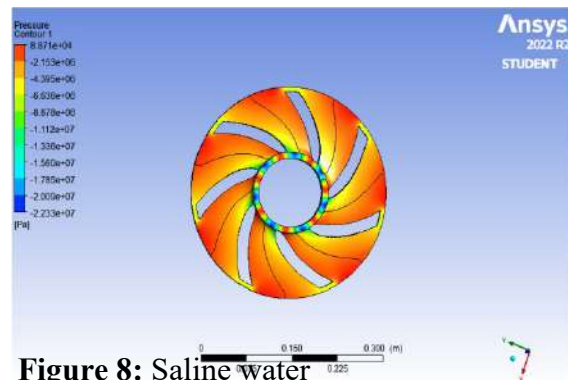
Figure 8: Saline water

Figure 9: Hydrochloric acid

Figure 7 – 9 depicts the pressure distribution across the impeller inlet angle of 38^0 and exit angle of 50^0 for various corrosive fluids.
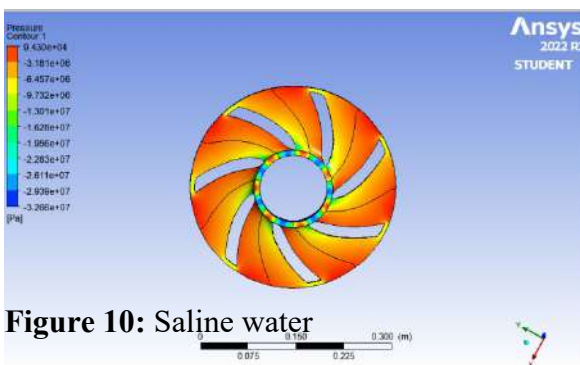
Figure 10: Saline water
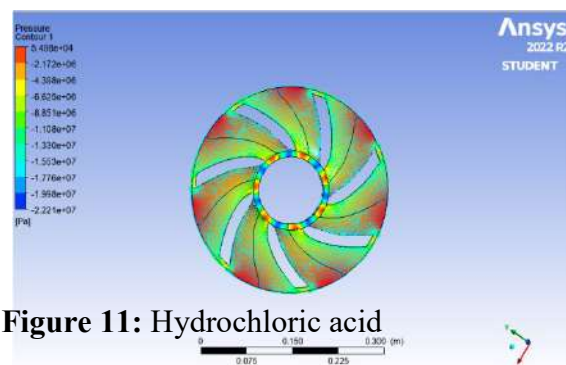
Figure 11: Hydrochloric acid
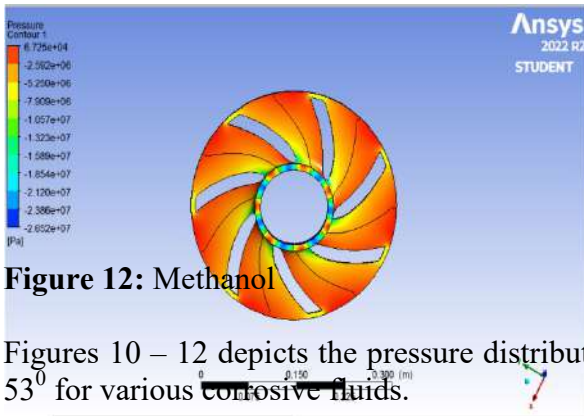
Figure 12: Methanol

Figures 10 – 12 depicts the pressure distribution across the impeller inlet angle of 41^0 and exit angle of 53^0 for various corrosive fluids.
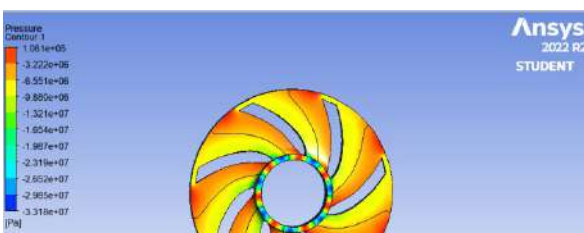
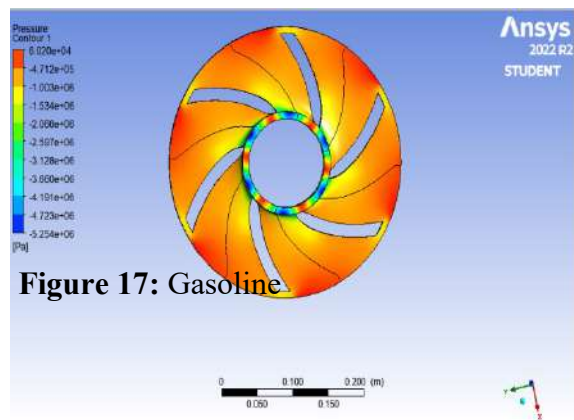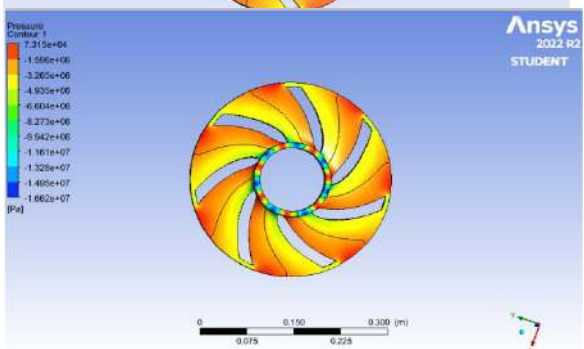**Figure 13:** Water at 100^oC
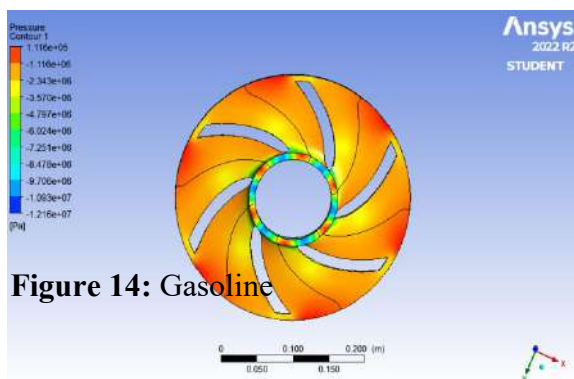
Figure 14: Gasoline
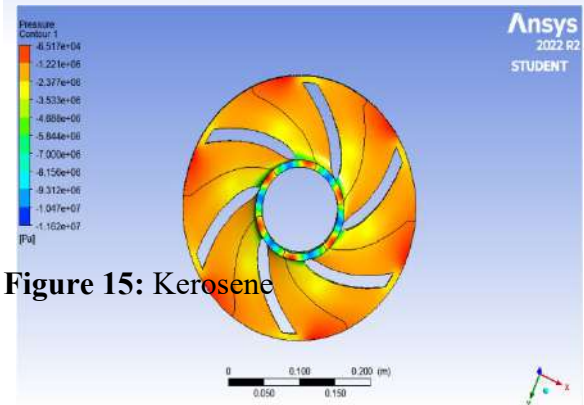
Figure 15: Kerosene

Figures 13 – 15 depicts the pressure distribution across the impeller inlet angle of 35^0 and exit angle of 47^0 for various non-corrosive fluids.
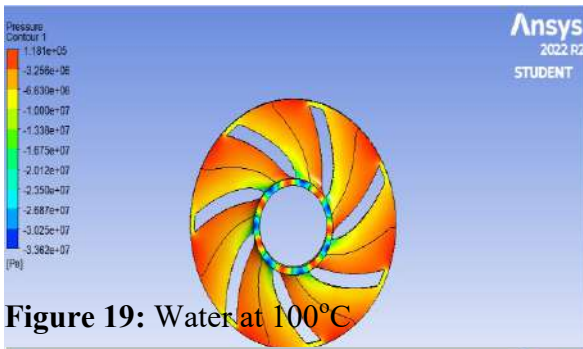

Figure 16: Water at 100^oC

Figure 17: Gasoline

Figure 18: Kerosene

Figures 16 – 18 depicts the pressure distribution across the impeller inlet angle of 38^0 and exit angle of 50^0 for various non-corrosive fluids.
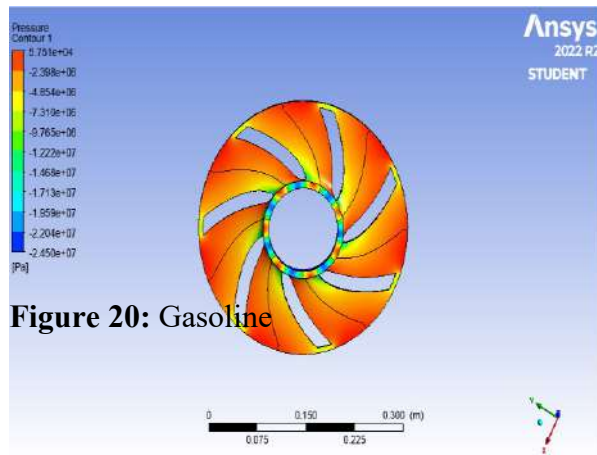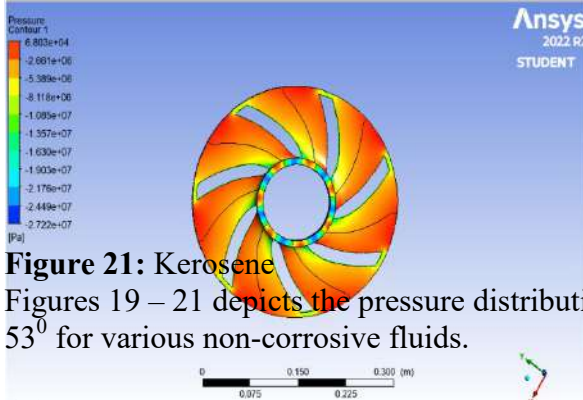

Figure 19: Water at 100°C

Figure 20: Gasoline

Figure 21: Kerosene

Figures 19 – 21 depicts the pressure distribution across the impeller inlet angle of 41^0 and exit angle of 53^0 for various non-corrosive fluids.
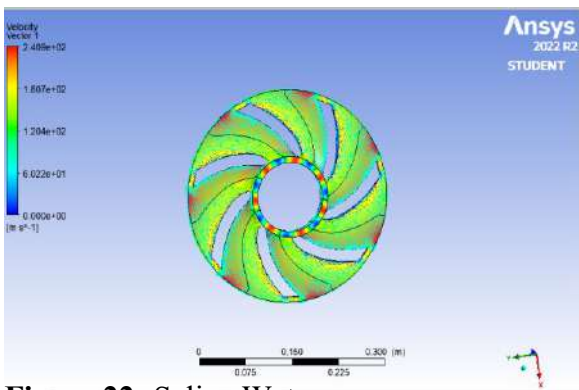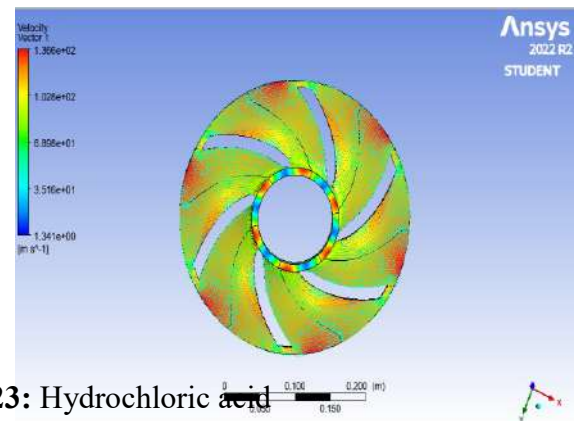
4.1.2 Relative Velocity Distributions
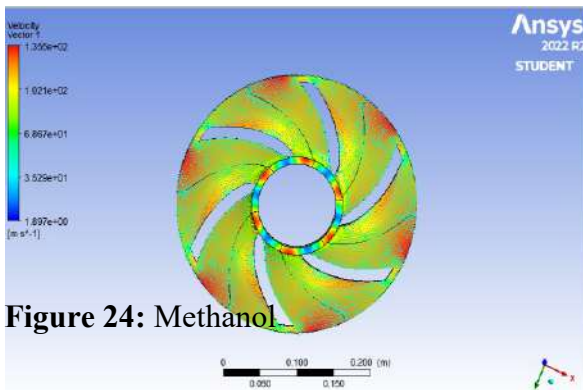

Figure 22: Saline Water

Figure 23: Hydrochloric acid

Figure 24: Methanol

Figures 22 – 24 depicts the relative velocity distribution at midspan of the impeller inlet angle of 35^0 and exit angle of 47^0 for various corrosive fluids.

Figure 25: Saline water

Figure 26: Hydrochloric acid

Figure 27: Methanol
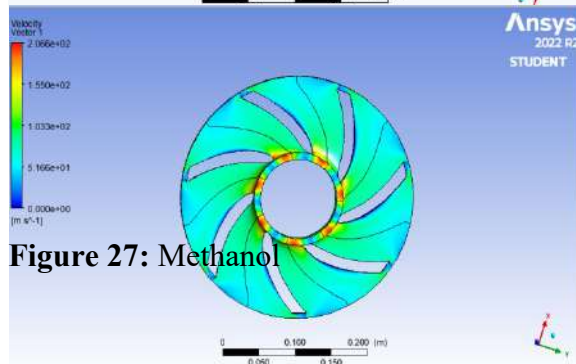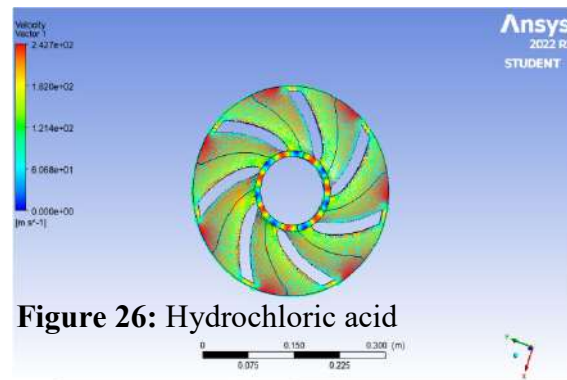
Figures 25 – 27 depicts the relative velocity distribution at midspan of the impeller inlet angle of 38^0 and exit angle of 50^0 for various corrosive fluids.
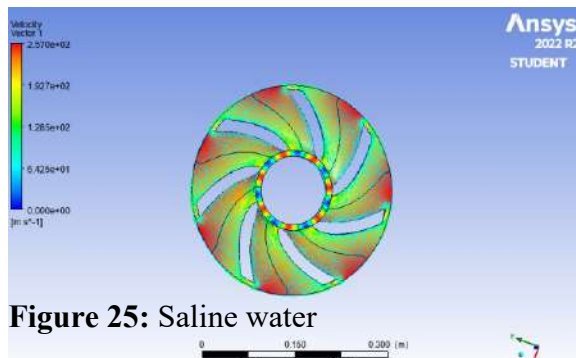

Figure 28: Saline water

Figure 29: Hydrochloric acid

Figure 30: Methanol

Figures 28 – 30 depicts the relative velocity distribution at midspan of the impeller inlet angle of 41^0 and exit angle of 53^0 for various corrosive fluids.
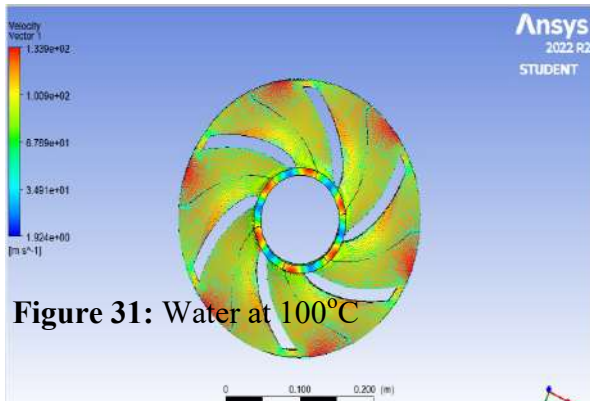
Figure 31: Water at 100°C
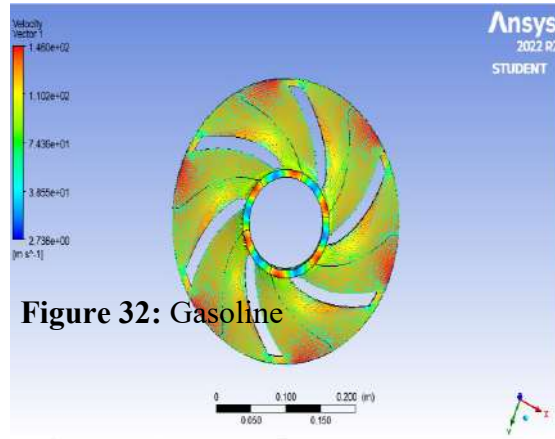
Figure 32: Gasoline
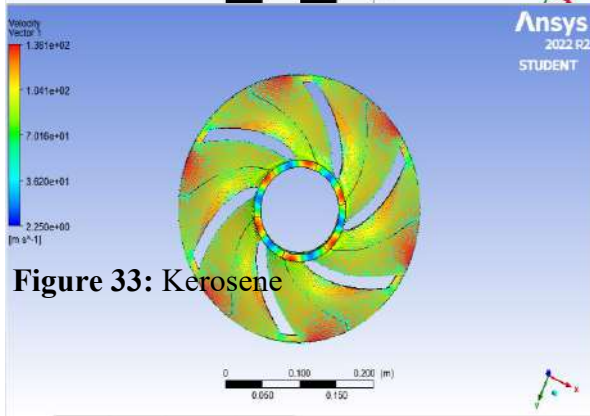
Figure 33: Kerosene
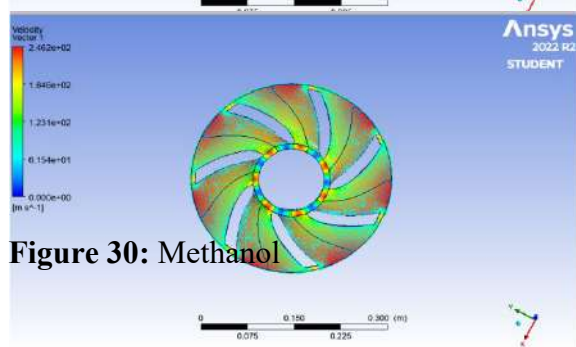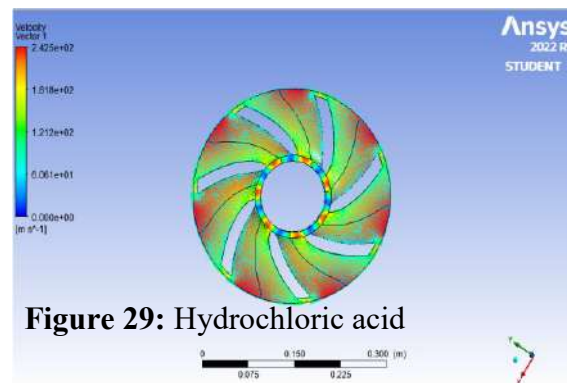
Figures 31 – 33 depicts the relative velocity distribution at midspan of the impeller inlet angle of 35^0 and exit angle of 47^0 for various non-corrosive fluids.

Figure 34: Water at 100°C

Figure 35: Gasoline
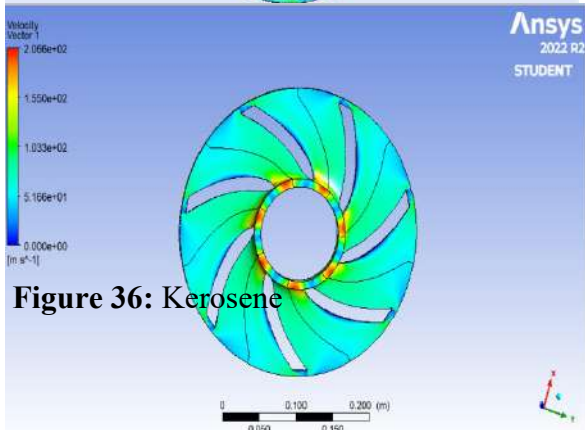
Figure 36: Kerosene

Figure 4.14: Relative velocity distribution at midspan of the impeller inlet angle of 38^0 and exit angle of 50^0 for various non-corrosive fluids.

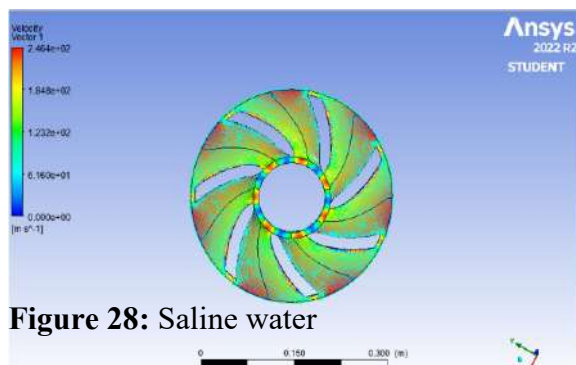**Figure 37:** Water at 100°C
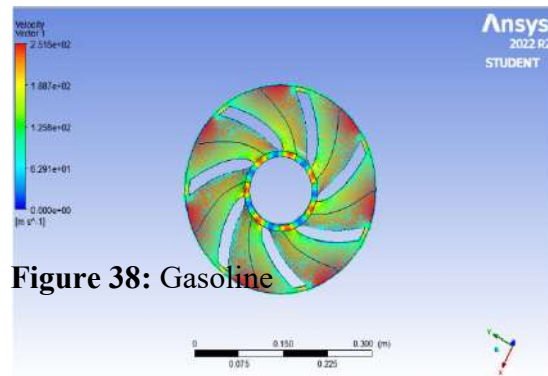
Figure 38: Gasoline
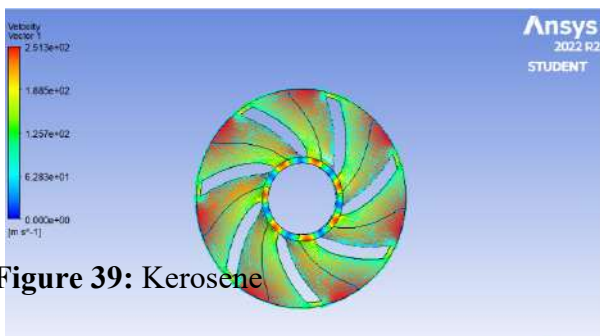
Figure 39: Kerosene

Figures 37 – 39 depicts the relative velocity distribution at midspan of the impeller inlet angle of 41^0 and exit angle of 53^0 for various non-corrosive fluids.
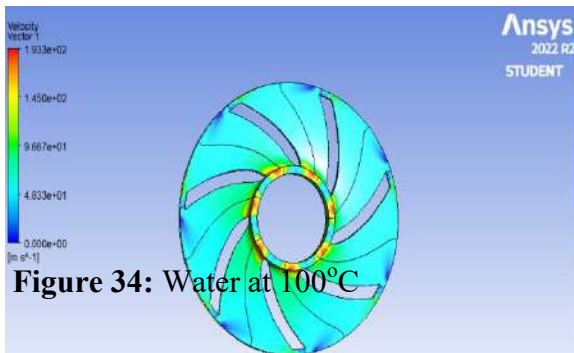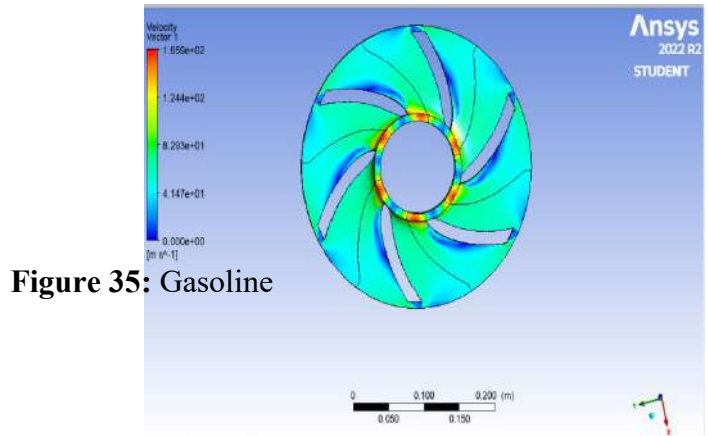
4.1.3 Performance Results of the Impeller for Corrosive and Non Corrosive Fluids at Different Impeller Inlet and Exit Angles.

Tables 4.1 and 4.2 respectively represent the power in kilowatt (kW) for each of the impeller and efficiency (%) for each of the impeller.

Table 4.1: Power in kilowatt (kW) for each of the impeller

Angles		Corrosive Fluids			Non-Corrosive Fluids		
Inlet	Outlet	Saline water	Hydrochloric Acid	Methanol	Water	Gasoline	Kerosene
				Power (kW)			
35^0	47^0	659..40	478.80	582.90	194.10	367.00	596.83
38^0	50^0	576.20	377.53	335.64	427.20	301.22	585.40
41^0	53^0	549.90	343.50	396.33	505.79	322.76	420.74

Table 4.2: Efficiency (%) for each of the impeller

Angles		Corrosive Fluids			Non-Corrosive Fluids		
Inlet	Outlet	Saline water	Hydrochloric Acid	Methanol	Water	Gasoline	Kerosene
				Efficiency (%)			

35^0	47^0	70.76	67.55	68.88	76.23	73.12	47.83
38^0	50^0	77.45	78.23	80.23	89.07	76.58	62.44
41^0	53^0	82.33	80.55	81.23	94.21	83.32	76.58

Figure 40: Performance curve for various corrosive fluids (a - c)

Figure 41: Performance curve for various non-corrosive fluids (a - c)

4.2 Discussion of Results

4.2.1 Pressure Distributions

The pressure distributions of impeller across the impeller inlet angle of 35^0 and exit angle of 47^0 for various corrosive fluids are shown in Fig. 4 - 6. The saline water, Hydrochloric acid, and Methanol corrosive fluids have inlet pressure of -33180kPa, -988kPa, -896kPa and outlet pressure of 106kPa, 541kPa and 665kPa respectively, and it can be seen in Fig. 7 – 9. Pressure distribution across the impeller inlet angle of 38^0 and exit angle of 50^0 for various corrosive fluids (saline water, Hydrochloric acid, and Methanol) have inlet pressure of -2233kPa, -1389kPa, -9807kPa and outlet pressure of 89kPa, 61kPa, 72kPa respectively. Hence, from Fig. 10 - 12, Pressure distribution across the impeller inlet angle of 35^0 and exit angle of 47^0 for various non-corrosive fluids (Water, Gasoline and Kerosene) have inlet pressure of -3318kPa, -1216kPa, -1421kPa and outlet pressure of 106kPa, 112kPa, 213kPa respectively. While from Fig 13 – 15. Pressure distribution across the impeller inlet angle of 38^0 and exit angle of 50^0 for Water, Gasoline and Kerosene have inlet pressure of -2148kPa, -5254Pa, -1662kPa and outlet pressure of 60kPa, 73kPa, 118kPa respectively. And can also can be seen from Fig. 13 – 15. Pressure distribution across the impeller inlet angle of 41^0 and exit angle of 53^0 for Water, Gasoline and Kerosene have inlet pressure of -3362kPa, -2450Pa, -2722kPa and outlet pressure of 118kPa, 58kPa, 68kPa respectively. Contours of static pressure and liquid flow velocity for designed impeller Q = 0.04 m^3/s for corrosive and non-corrosive fluids can be seen that the pressure and velocity is higher for non-corrosive fluids than that of the corrosive fluids. The static difference between impeller inlet and outlet increases with large exit blade angle. This happens because of fluid flow velocity at impeller outlet, which decreases with increase in discharge angle. The contours depict a smooth flow and the pressure increases continuously towards the exit of the domain. The lowest static pressure can be observed at the impeller inlet on suction side (Han et al; 2018)

It can be seen that the pressure gradually increases from the impeller inlet to outlet; the pressure at the inlet has the smallest value and a large gradient. The pressure is bigger on the pressure surface than that on the suction surface at the same position, so the back surface of inlet is the position where cavitation is prone to occurrence. Due to the obstruction effect, the pressure of the tongue part will have some certain fluctuations. By comparing the pressure distributions in Figs. 4 - 6, 7 - 7, 8 - 10, 11 - 13 and 14 - 16, it can be concluded that the pressure of impeller inlet first decreases and then increases, and the change trend of pressure distribution is consistent under different inlet and outlet angles and different corrosive and non-corrosive fluids. Note that the pressure near the tongue will increase with the increase of the blade outlet angle at low flow rate condition.

4.2.2 Relative Velocity Distribution

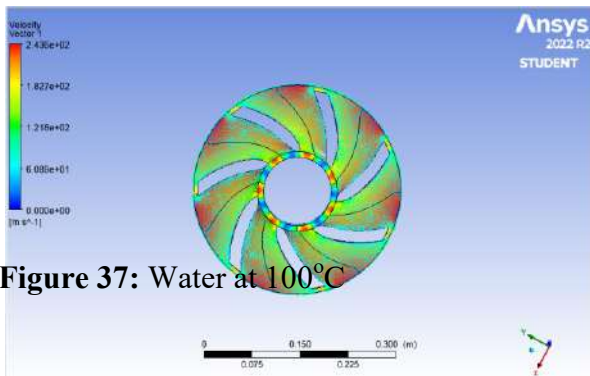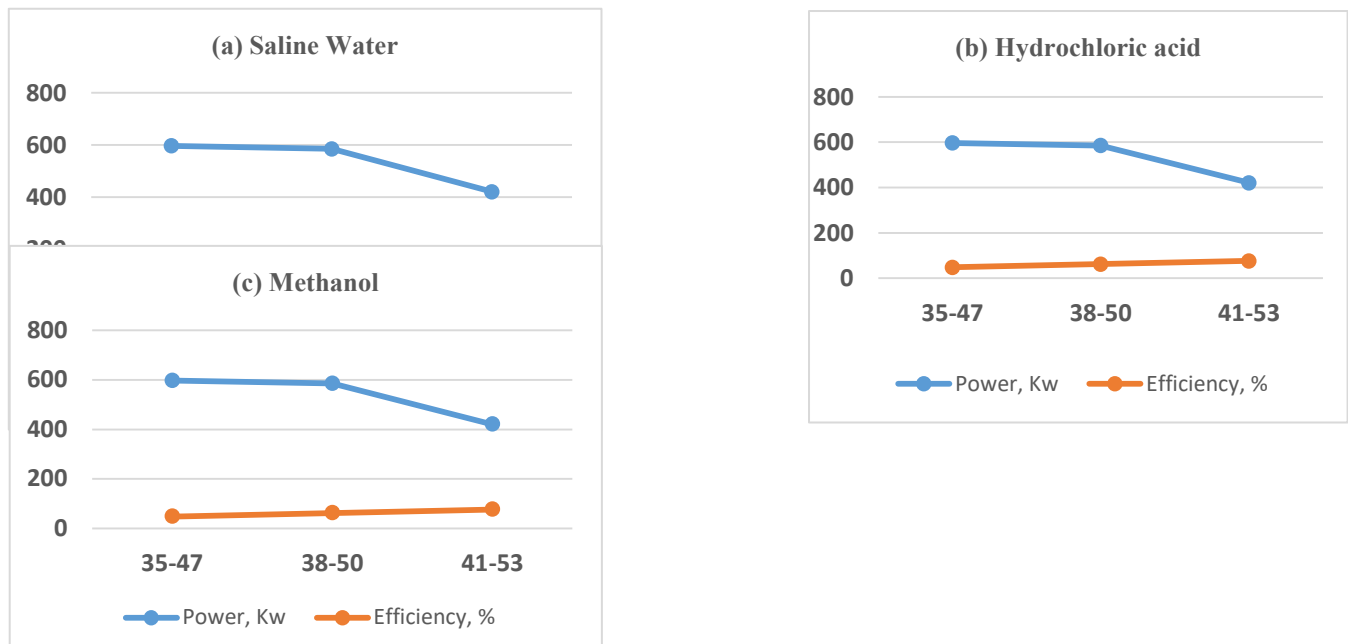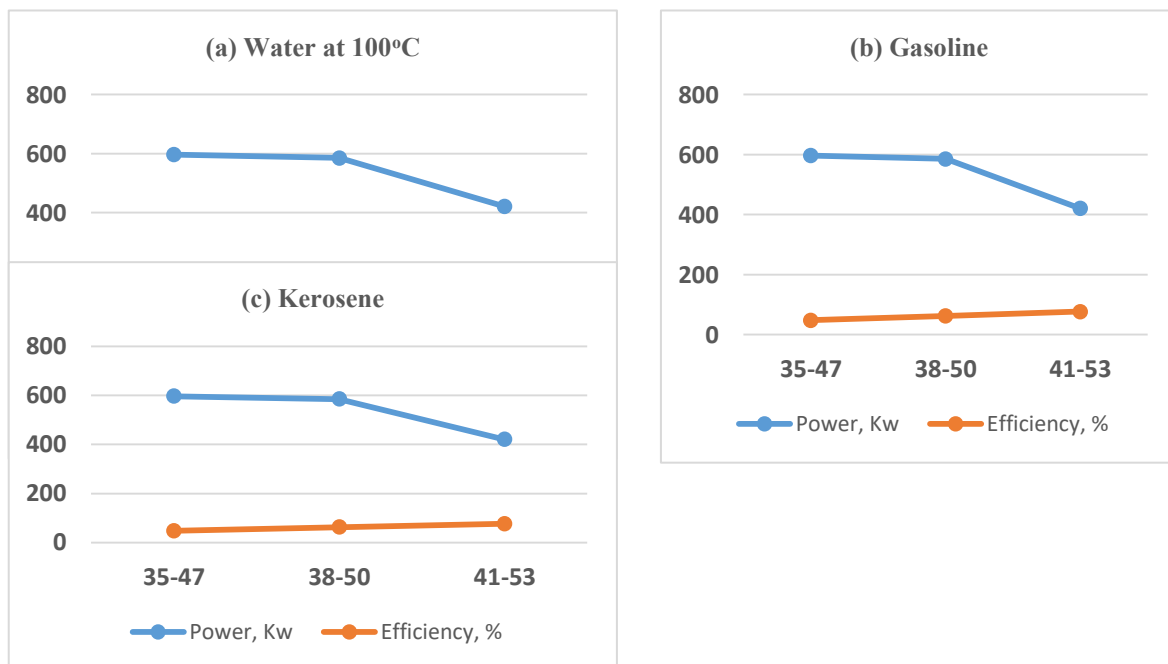Fig. 4.10 shows the relative velocity distribution of the at midspan of the impeller inlet angle of 35^0 and exit angle of 47^0 for various corrosive fluids Saline water, Hydrochloric acid and methanol which have velocity at the impeller inlet of 0.00m/s, 1.34m/s, 1.9m/s and outlet velocity of 241m/s, 137m/s, 136m/s respectively. Also from Fig. 4 - 6, the relative velocity distribution of the impeller inlet angle of 38^0 and exit angle of 50^0 for Saline water, Hydrochloric acid and methanol have velocity at the impeller inlet of 0m/s and outlet velocity of 257m/s, 243m/s, 207m/s respectively.

As well for inlet blade angle of 41^0 and outlet blade angle of 53^0 in Fig. 7 - 9 the inlet velocity for various fluids are 0m/s and outlet velocity of 246m/s, 243m/s, 246m/s respectively.

Hence, for non-corrosive fluids (Water, Gasoline and Kerosene) in Fig. 10 - 12 for blade inlet angle of 35^0 and exit blade angle of 47^0 the inlet velocity of 1.9m/s, 2.7m/s, 2.3m/s from suction side and exit velocity of 134m/s, 146m/s, 138m/s respectively. And from Fig. 13 - 15, the relative velocity distribution across the impeller inlet angle of 38^0, 41^0 and exit blade angle of 50^0, 53^0 respectively for Water, Gasoline and Kerosene fluids have inlet velocity of 0m/s and exit velocity of 193m/s, 166m/s,

207m/s and 244m/s, 252m/s, 251m/s respectively. It can be seen that the relative velocity of the fluid in the impeller increases gradually, and the velocity has minimum value and smaller gradient in uniform flow at the impeller inlet. At the impeller outlet, with the rise of blade outlet angle, the flow velocity increases and the flow becomes unstable, and the velocity at the pressure surface is bigger than that on the back. At the inlet of the impeller, the relative velocity was small. At the outlet of the impeller, the relative velocity attained the maximum, which was in agreement with the experimental and theoretical results. Relative velocity in the pressure surface was much smaller than that of suction pressure.

4.2.3 Performance of the Impeller at Different Blade Inlet and Outlet Angle of Different Corrosive and Non-Corrosive Fluids.

The performance curve for corrosive fluids at different inlet and outlet angles of the impeller is shown in figure 4.16, it can be seen that for saline water the shaft power of the impeller angle of 35^0 - 47^0 the efficiency is increasing while for the impeller of 38^0 - 50^0 inlet and outlet angle the power is reducing, hence the efficiency is gradually increasing and for the impeller of 41^0 - 53^0 the shaft power had continuous decrease while the efficiency attained maximum. Therefore, for Hydrochloric acid yield the same results as that of Saline water but hydrochloric acid has maximum efficiency.

The performance curve for various non-corrosive fluids at different inlet and outlet angles of the impeller is shown in figure 16 - 18, it can be seen that for water at 100 degree Celsius at the certain shaft power of the impeller angle of 35^0 - 47^0 the efficiency is had also increased while for the impeller of 38^0 - 50^0 inlet and outlet angle the power is reduced, hence the efficiency is gradually increasing and for the impeller of 41^0 - 53^0 the shaft power had continuous decrease while the efficiency attained maximum. Therefore, Gasoline and kerosene had also yield the same results as that of water at 100 degrees Celsius which has maximum efficiency. Which proved that the higher the efficiency, the less energy required to operate for a specific performance point (Zhou et al., 2013).

The overall efficiency of the impellers was calculated based on both shaft powers which operate at 2000 rpm and different mass flowrate for both corrosive and non-corrosive fluids. For the same flow rate and discharge angle, the input power is more for denser fluids (Bellary & Samad, 2016). The increase in flow rate results in increase in power consumption. The density of water, gasoline and kerosene is lesser than that of saline water, methanol and hydrochloric acid saline, which causes the lesser power consumption. Higher inlet and exit angle, the power consumption by the impeller is increased. A large exit angle favours efficiency improvement. When selecting the best pump for application, impeller efficiency is of more paramount factor to be considered.

5.0   Conclusion and Recommendation

5.1 Conclusion

In this research, the improvement on reliability and efficiency of centrifugal pump impeller performance at discharge of 0.04m^3/s and head rise of 50 - 75 different mass flow rates have been evaluated by numerical simulations using ANSYS software for corrosive (Saline water, Hydrochloric acid, Methanol) and non-corrosive (Water at 100^0C, Gasoline, Kerosene) fluids.

1) The centrifugal pump impeller received the necessary materials from ANSYS software material library in accordance with the requirement and features.
2) The pressure distribution at the inlet is less and large slope, and the pressure at the outlet increases with the increase of the blade outlet angle at different flowrate which create some certain fluctuations.
3) The velocity distribution of the impeller near the suction side has is relatively small while at the exit increased with increase blade inlet and outlet angle for various fluids at different mass flow rate.
4) The density of water, gasoline and kerosene is lesser than that of saline water, methanol and hydrochloric acid saline, which causes the lesser power consumption. Higher inlet and exit angle,

the power consumption by the impeller is increased. After the study Hydrochloric acid and water has a maximum efficiency.

5.2 Recommendation

Despite the fact that the analysis covered a lot of ground, certain limitation necessitates future consideration of the design of a new impeller, leading to the following recommendations:

1.) It is important to conduct more research on the impeller with volute to determine the surface roughness and its effect using corrosive fluids.
2.) To verify the numerical result and analysis, the performance test apparatus for the centrifugal pumps should be designed and built for further researches.
3.) The same working constraints should be used to establish the functionality of the material.

6.0 Reference

Bellary, S. A. I., & Samad, A. (2016). Pumping crude oil by centrifugal impeller having different blade angles and surface roughness. *Journal of Petroleum Exploration and Production Technology*, *6*(1), 117–127. https://doi.org/10.1007/s13202-015-0173-y

Flows, T., Jiang, Q., Heng, Y., Liu, X., Zhang, W., & Bois, G. (2019). A Review of Design Considerations of Centrifugal Pump Capability for Handling Inlet Gas-Liquid. https://doi.org/10.3390/en12061078

Han, X., Kang, Y., Li, D., & Zhao, W. (2018). Impeller optimized design of the centrifugal pump: A numerical and experimental investigation. *Energies*, *11*(6). https://doi.org/10.3390/en11061444

Idris M. N., and Umaru I. U., (2023), 'Experimental studies and designs using corrosive and non-corrosive materials to improve on reliability and efficiency of an impeller of a centrifugal pump.' Unpublished *final year research Thesis submitted to the Department of Chemical Engineering, University of Maiduguri. Borno State Nigeria*

Idris M. N., and Kois A. A., (2022), 'Application of CFD to Improve on Reliability and Efficiency of Centrifugal Pump for Oil and Gas Processing Plant' *African Journal of Engineering and Environmental Research (AJEER)*, ISSN 2635-2974 Vol. 3 No. 1. Pages 128 – 143. https://ajoeer.org.ng

Ji, P. E. I., Wenjie, W., Shouqi, Y., & Jinfeng, Z. (2016). Optimization on the Impeller of a Low-specific-speed Centrifugal Pump for Hydraulic Performance Improvement. https://doi.org/10.3901/CJME.2016.0519.069

Karmokar, S. (2019). Wear Rate Comparison of Different Impeller Materials for Pumping Various Types of Slurry. May.

Li, X., Chen, H., Chen, B., Luo, X., Yang, B., & Zhu, Z. (2020). Investigation of fl ow pattern and hydraulic performance of a centrifugal pump impeller through the PIV method. *Renewable Energy*, *162*, 561–574. https://doi.org/10.1016/j.renene.2020.08.103

Pradesh, A. (2017). Design and Analysis of Centrifugal Water Pump Impeller Made of Polyphelene Sulphide Material. 5762, 170–175.

Rajendran, S., & Purushothaman, K. (2012). Analysis of a centrifugal pump impeller using ANSYS-CFX. *Ijert*, *1*(3), 1–6. https://doi.org/10.15680/IJIRSET.2018.0705025

Selamat-, F. E. (2018). Design and Analysis of Centrifugal Pump Impeller for Performance Enhancement. *5*(2), 36–53.

Selamat, F. E., Wan Izhan, W. H. I., & Baharudin, B. S. (2018). Design and analysis of centrifugal pump impeller for performance enhancement. *Journal of Mechanical Engineering*, *5*(Specialissue2), 36–53.

Zhou, L., Shi, W., & Wu, S. (2013). Performance Optimization in a Centrifugal Pump Impeller by Orthogonal Experiment and Numerical Simulation. *2013*. https://doi.org/10.1155/2013/385809